Design of Scaled Prototypes of EMS Maglev Levitators, Based on an Improved Magnetic Modelling

CASTELLI DEZZA, Francesco, DI GERLANDO, Antonino, FOGLIA, GianMaria
Dipartimento di Elettrotecnica - Politecnico di Milano
Piazza Leonardo da Vinci 32, 20133 Milano, Italy
Phones: +39 02 239937/12-22-52, Fax: +39 02 23993703
E-Mails: [francesco.castellidezza, antonino.digerlando, gianmaria.foglia]@polimi.it

Keywords : EMS Maglev, EMS Maglev design.

Abstract
This paper describes the design steps of two types of Maglev levitators, the first equipped with coils only and the other hybrid (coils + permanent magnets); the design has two features:
– the studied levitator is conceived in electromagnetic similitude with a real one;
– the design is based on an improved modelling of the quantities concerning the air-gap.
After the analysis of the criteria used for the similitude, the paper shows the design of the two levitator types.

1. Similitude Theory

Within the research on EMS Maglev electric systems for transportation, in progress c/o the Department of Electrical Engineering of *Politecnico di Milano*, it seemed to be worthwhile to construct some levitators in similitude towards those of real vehicles, to carry out tests giving as much as possible representative results, without operating on a full scale dimension vehicle.
Once decided the construction of a levitator in scale with the Transrapid sizes, we needed to choose the basic criteria to set the dimensions of the object. It seemed to be suitable to greatly reduce the weight (by a factor 0.1), and to assume a lower reduction for the longitudinal dimensions (by a factor 0.4); we decided to maintain the same main physical quantities of the real levitator (average flux density under the pole, B_δ, and rated current density in the coils, J_n [1]), and the same mechanical dynamics (that is the same vertical acceleration $\ddot{\delta}$), in such a way to stimulate the electromechanical system similarly to the real levitator.
Hereafter, we first show how impose the chosen conditions, subsequently which constraints they produce on the transversal sizes and on the air-gap, and finally their effects on the system electrical dynamics.
Considering the levitator scheme shown in fig. 1.1, we assume:

F = magnetic attractive levitation force
P = weight lifted by one levitator
$m = P/g$ = mass lifted by one levitator
τ, τ_c = pole pitch, slot pitch
b_e = pole shoe longitudinal width
b_p = pole body longitudinal width
ℓ = transversal dimension of pole shoe and stator
δ = air-gap width
$\ddot{\delta}$ = vertical acceleration ($d^2\delta/dt^2$)
J = current density in windings
B_δ = air-gap flux density (average flux density under pole shoe = ratio of magnetic flux at the air-gap and the geometric pole shoe cross section)
$H_\delta = B_\delta / \mu_0$ = magnetic field in the air-gap
A_{Cu} = copper net total area
h_b, b_b = coil size height and width
$A_b = h_b \cdot b_b$ = coil size area
$\alpha_{Cu} = A_{Cu} / A_b$ = copper filling factor

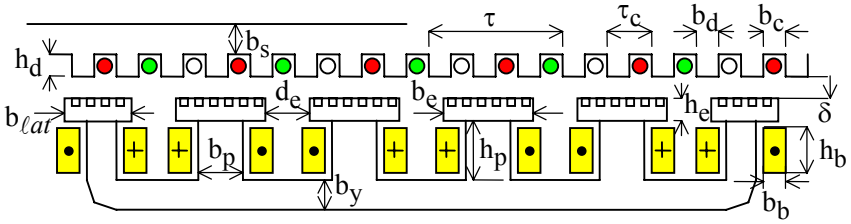

Fig. 1.1: schematic structure and main sizes of a Transrapid type levitator.

[1] We notice that assuming the same current density supposes the same cooling conditions; this is not completely true in the reduced dimensions levitator, as the considered platform is "static" (it does not run).

All the previously defined quantities have the subscript "rid" if referred to the reduced sizes structure.
The following reduction coefficients are defined:

$\alpha_F = F_{rid}/F = P_{rid}/P = (m_{rid}\,g)/(mg) = m_{rid}/m$: force, weight, mass reduction coefficient;

$\alpha_\tau = \tau_{rid}/\tau = b_{e\,rid}/b_e = b_{b\,rid}/b_b = b_{p\,rid}/b_p$: longitudinal dimensions reduction coefficient (polar pitch, polar shoe width, coil width, polar body width)

$\alpha_\ell = \ell_{rid}/\ell$: transversal dimensions reduction coefficient;

$\alpha_\delta = \delta_{rid}/\delta$: air-gap reduction coefficient.

The constraint concerning the mechanical dynamics is already verified, as $\ddot{\delta}_{rid} = \ddot{\delta}$:

$$\frac{\ddot{\delta}_{rid}}{\ddot{\delta}} = \frac{F_{rid}/m_{rid} - g}{F/m - g} = \frac{(\alpha_F \cdot F)/(\alpha_F \cdot m) - g}{F/m - g} = 1\,.$$

The constraints about weight and longitudinal dimensions are simply: $\alpha_F = 0.1$ and $\alpha_\tau = 0.4$.

As regards α_ℓ, we observe that the dimension ℓ can be expressed as a function of the following quantities: per pole levitation force, flux density and pole shoe width b_e: $\ell = F/\left(b_e \cdot B_\delta^{\,2}/(2\mu_0)\right)$.

Then, considering that the flux density is the same in the real structure and in the reduced one, we have:

$$\alpha_\ell = \frac{\ell_{rid}}{\ell} = \frac{F_{rid}\Big/\frac{1}{2\mu_0}B_\delta^{\,2}b_{e\,rid}}{F\Big/\frac{1}{2\mu_0}B_\delta^{\,2}b_e} = \frac{F_{rid}}{F}\frac{b_e}{b_{e\,rid}} = \frac{\alpha_F}{\alpha_\tau}\,.$$

About α_δ, we observe that the air-gap width can be obtained from the magnetic voltage loop law: neglecting the ferromagnetic voltage drops, we have: $H_\delta \cdot \delta = J \cdot A_{Cu}$, from which: $\delta = A_{Cu} \cdot J/H_\delta = \mu_0 \cdot A_{Cu} \cdot J/B_\delta$.

Considering that also the current density is the same in the real structure and in the scaled one, it follows:

$$\alpha_\delta = \frac{\delta_{rid}}{\delta} = \frac{\mu_0 J/B_\delta\, A_{Cu\,rid}}{\mu_0 J/B_\delta\, A_{Cu}} = \frac{A_{Cu\,rid}}{A_{Cu}}\,;$$

thus, α_δ equals the copper sections ratio. If we assume unvaried the coil copper filling factor, we can write:

$$\alpha_\delta = \frac{A_{Cu\,rid}}{A_{Cu}} = \frac{A_{b\,rid}/\alpha_{Cu}}{A_b/\alpha_{Cu}} = \frac{h_{b\,rid}\,b_{b\,rid}}{h_b b_b} = \frac{h_{b\,rid}}{h_b}\alpha_\tau\,.$$

If we reduced all the dimensions in a scaled way, also $h_{b_{rid}}/h_b$ ratio would equals α_τ, and so $\alpha_\delta = \alpha_\tau^{\,2}$: this relation is not acceptable, because it leads to a too much reduced air-gap width. F.e.: in an actual vehicle with a rated air-gap $\delta_n = 10$ mm and pole pitch $\tau = 300$ mm, supposing $\alpha_\tau = 0.5$, we would get $\alpha_\delta = \alpha_\tau^{\,2} = 0.25$, that is a rated air-gap of 2.5 mm: this is a very little value, hardly compatible with the mechanical tolerances and scarcely manageable by the levitation control system.

If we decide to fix α_δ, in order to avoid this problem, then the ratio $h_{b_{rid}}/h_b = \alpha_\delta/\alpha_\tau$ is fixed. F.e.: if $\alpha_\delta = \alpha_\tau$, we have $h_{b_{rid}} = h_b$, which means that the coils (and so the polar bodies) have the same height in the reduced structure and in the actual one.

Starting from some data concerning the Transrapid [6, pag. 315], [7, pag. 395-398], the characteristics reported in Table 1.2 and the dimensions shown in the central column of Table 1.1 have been adopted as reference values for the real vehicle. We decided to fix $\alpha_\delta = \alpha_\tau = 0.4$, from which $\alpha_\ell = 0.25$, resulting in the sizes of the right column of Table 1.1; Table 1.2 characteristics were assumed equal to those of the real vehicle.

Table 1.1: real vehicle versus platform characteristics

Quantity		*Real vehicle*	*Scaled platform*
m (1)	[kg]	2400	240
τ	[mm]	300	120
b_e	[mm]	200	80
ℓ	[mm]	240	60
δ_n	[mm]	10	4
τ_c	[mm]	100	40

(1) m is the mass concerning one esapolar levitator

Table 1.2: common characteristics of real vehicle and scaled platform

N° slots/(pole-phase)	1
Slot width / slot pitch	0.5
Slot height/ slot pitch	0.5

Now we analyse the consequences of the previous choices on the electrical dynamics. We assume:

L, R = winding inductance and resistance
$\tau_{elect} = L / R$ = circuit time constant
I = current RMS value
$A_{fe} = b_p \cdot \ell$ polar body section area
N = winding turn number
B_{fe} = polar body average flux density
$\varphi = B_{fe} \cdot A_{fe}$ = pole flux
$\psi = N \cdot \varphi = L \cdot I$ = flux linkage
$NI = JA_{Cu}$ = winding total current
ρ_{Cu} = copper resistivity
$L_{Cu} = 2 \cdot (b_p + \ell + 2b_b)$ = mean turn length
$Vol_{Cu} = A_{Cu} \cdot L_{Cu}$ = coil copper volume.

With these assumptions, we have:

$$\frac{\tau_{elect\,rid}}{\tau_{elect}} = \frac{(L/R)_{rid}}{L/R} = \frac{\left(LI^2/RI^2\right)_{rid}}{LI^2/RI^2} = \frac{\left(\psi I/\rho_{Cu}J^2 Vol_{Cu}\right)_{rid}}{\psi I/\rho_{Cu}J^2 Vol_{Cu}} = \frac{\left(\varphi NI/\rho_{Cu}J^2 A_{Cu}L_{Cu}\right)_{rid}}{\varphi NI/\rho_{Cu}J^2 A_{Cu}L_{Cu}} =$$

$$= \frac{\left(B_{fe}A_{fe}JA_{Cu}/\rho_{Cu}J^2 A_{Cu}L_{Cu}\right)_{rid}}{B_{fe}A_{fe}JA_{Cu}/\rho_{Cu}J^2 A_{Cu}L_{Cu}} = \frac{\left(B_{fe}A_{fe}/\rho_{Cu}JL_{Cu}\right)_{rid}}{B_{fe}A_{fe}/\rho_{Cu}JL_{Cu}} = \frac{\left(A_{fe}/L_{Cu}\right)_{rid}}{A_{fe}/L_{Cu}} = \frac{\left(b_p\ell/2\left(b_p+\ell+2b_b\right)\right)_{rid}}{b_p\ell/2\left(b_p+\ell+2b_b\right)}$$

$$\Rightarrow \frac{\tau_{elect\,rid}}{\tau_{elect}} = \frac{\left(b_p\ell\right)_{rid}}{b_p\ell}\frac{\left(b_p+\ell+2b_b\right)}{\left(b_p+\ell+2b_b\right)_{rid}} = \alpha_\tau\alpha_\ell\frac{b_p+\ell+2b_b}{\alpha_\tau b_p+\alpha_\ell\ell+2\alpha_\tau b_b}$$

With the chosen values ($\alpha_\tau = 0.4$, $\alpha_\ell = 0.25$) and the Table 2.2 data (ℓ = 240 mm, τ = 300 mm, b_e = 200 mm), assuming preliminarily $b_p = b_e/2$ = 100 mm and $b_b = (\tau - b_p)/2$ = 100 mm, we obtain $\tau_{elect\,rid} / \tau_{elect} = 0.3$, that is the reduced levitator time constant equals 30% that of the real levitator one. Obviously, this result is not rigorously exact, because of the substantial simplifications adopted (first of all, in inductance calculation, we neglected leakage flux, fringing, and border effect); nevertheless, in qualitative terms, it is true that the duration of the electrical transients is higher in the real levitator, thus the real levitation control may be more difficult, because more time is needed to get the steady-state condition (with the same electrical source); for this reason, in the real system, an increment of the coil feeding converter DC bus voltage could be required.

Note: all the observations concerning the similitude should refer, strictly speaking, only to the levitator with coils only, as the Transrapid system belongs to this type; in practice, they can be extended to the hybrid levitator equipped with permanent magnets, as we decided to assume for the hybrid levitator the same main sizes (air-gap quantities and transversal dimension) of the levitator with coils only.

2. Levitator Design

The Definition of the Main Physical Quantities.

As already explained, our initial intent was to maintain the same main physical quantities of the Transrapid levitator (average flux density under the pole shoe B_δ and rated current density in the winding J_n); but it was not possible to find detailed information concerning these data in literature, so the choice of the main physical quantities concerning the reduced scale prototype was made on the basis of other factors.
Due to the high air-gap, it is worthwhile to assume a low value of the air-gap flux density, to limit Joule losses in levitation windings. In fact, the high speed and mass of the running vehicle and the inherent instability of the equilibrium among levitation force and vehicle weight, suggest to choose the air-gap width not under about ten millimetres, for safety reasons. This value, which is very little from a mechanical viewpoint, is instead high in magnetic terms: in this system, the ratio between air-gap and equivalent magnetic length of the ferromagnetic core is much higher than that usually occurring in traditional magnetic structures. If we consider that the air-gap flux density is roughly proportional to the m.m.f. and inversely proportional to air-gap width, it follows that, as the air-gap increases, it is needed to proportionally increase the m.m.f., or to reduce the flux density. In Maglev levitators, a limitation of the m.m.f. is required in order to lower winding Joule losses; thus, suitable air-gap flux density values should not exceed 0.5÷0.6 T (average value of air-gap flux density, i.e. ratio of air-gap pole flux and pole shoe geometrical section area); we assumed B_δ = 0.55 T.
As regards the current density, on the basis of the weak cooling conditions (air natural convection thermal exchange, considering that the platform does not run), the value must be low: we assumed J_n = 4 A/mm^2.
About the design value of the core flux density B_{fe}, it is prudent to adopt a low value, to ensure operation far from saturation conditions, in such a way to maintain a good regulation margin to the control system. In fact:

– the system is characterised by different elements which make the control difficult: inherent instability (weight – levitation force dynamic equilibrium), high mass and speed, not linear links between variables (force – air-gap and force – current links), time varying parameters. It is advisable not to add another difficulty, that is the non linearity of B – H link too near to the saturation zone;
– if ferromagnetic material operates near saturation, and an increase of force is required (e.g., to oppose an incipient air-gap increase, due to a perturbation), very high m.m.f.s are necessary to get the desired flux (and so force) increase, and the feeding system has to satisfy these request; instead, if a lowering of force is needed, the m.m.f. reduction is very low: thus, the feeding conditions are highly non symmetrical; these facts increase the difficulty of the levitation control. Instead, if core operates far from saturation, the m.m.f. variations are limited, and roughly symmetrical in the two directions.

We adopted $B_{fe} = 1.4$ T.

Improved Model

We said that one of the peculiarities of the system is the use of an improved model of the equivalent magnetic circuit (this model is described in detail in [5]). Following this model, the air-gap quantities (fluxes and forces) are calculated as the product of some ideal quantities times suited correction coefficients.
Ideal quantities are those concerning a uniform magnetic field (that is, the field developing between two parallel, unlimited, smoothed structures); ideal quantities expressions are therefore:

$$\varphi_{id} = A \cdot B_{id} \quad , \qquad F_{id} = A \cdot B_{id}^{\,2} / (2\mu_0) \quad , \qquad B_{id} = \mu_0 \cdot U / g \, ,$$

where the symbols have the following meaning: B_{id} = uniform field flux density; U = magnetic voltage drop between the two ferromagnetic structures; A = considered surface portion; g = air-gap between structures.
Correction coefficients give the ratio between the value of a magnetic quantity in a real structure, and the corresponding value of the same quantity in the ideal field; in this way, considering any magnetic structure, each magnetic quantity can be simply and rapidly calculated as a product of the ideal quantity times the corresponding correction coefficient; based on this definition, the expressions of the real quantities are simply:

$$\phi = B_i \cdot A_{geom} \cdot k_\varphi \, , \quad \phi = \mu_0 \frac{U_\delta}{\delta} \cdot A_{geom} \cdot k_\varphi \, , \quad F = \frac{1}{2\mu_0} \cdot B_i^2 \cdot A_{geom} \cdot k_F \, , \quad F = \frac{1}{2\mu_0} \left(\mu_0 \frac{U_\delta}{\delta} \right)^2 \cdot A_{geom} \cdot k_F \, .$$

The correction coefficients are analytical functions of the structure geometrical dimensions; their origin and expressions are described in detail in [1].

Choice Criteria of the Ideal Flux Density B_i

Levitator geometrical dimensions can be obtained from fluxes and forces expressions only if the ideal flux density value B_i is known: so, first of all, a B_i value must be chosen. This value must observe the constraint concerning the air-gap flux density limitation: therefore, the ideal flux density B_i has to be linked to the air-gap flux density of the real structure B_δ. This link is found considering that, by definition, $B_\delta = \phi / A_{geom}$ (in fact, B_δ is the mean value of air-gap flux density, that is the ratio of air-gap pole flux and pole shoe geometrical section area) and $\phi = B_i \cdot A_{geom} \cdot k_\varphi$, from which $B_\delta = B_i \cdot k_\varphi$ and therefore $B_i = B_\delta / k_\varphi$ (*).

We observe that the found link is a consequence of comparing the flux expressions; in a similar way, force expressions could be compared, resulting in a different link:

$$F = \frac{1}{2\mu_0} B^{*2} A_{geom} = \frac{1}{2\mu_0} \cdot B_i^2 \cdot A_{geom} \cdot k_F \qquad \Rightarrow \qquad B_i = B^* / \sqrt{k_F} \quad (**).$$

In this case, the link occurs between the ideal flux density B_i and a particular value of flux density B^*, related to force expression. In our case, the constraint concerning the low air-gap flux density involves the quantity B_δ, and so the use of the link (*) is correct; on the contrary, if the only aim were to obtain a given force, the quantity B^* would be involved, and the link (**) should be used.

2.1 Design of the Levitator with Coils Only

2.1.1 Choice of the Parameters σ_δ and ℓ

Referring to fig. 1.1, we call: $\sigma_\delta = b_{\ell at} / b_e$ the ratio between the longitudinal extension of the esapolar levitator lateral pole shoe and the extension of the internal pole shoe; ℓ is the transversal size of the levitator.
The choice of such parameters is based on the following aims:

– for simplicity and symmetry reasons, it is worthwhile that all the coils produce the same m.m.f. value;
– at rated condition, the levitator has to generate the rated levitation force;
– stator flux equilibrium is desired, that is we want that the flux is the same in every stator yoke section, and equal to one half the flux in each central pole; this fact quite exclusively depends on the lateral pole shoe extension: if this extension equals the central pole shoe extension, the system operates in a mode that can be called "independent magnetic loop" operation (fluxes come out from each pole and returns through only one of the adjacent poles, see fig. 2.1.1); the result is that some stator yoke sections are crossed by the total pole flux, and no flux runs through the adjacent sections: in this case, the stator yoke must carry the total pole flux (instead of one half), and this requires a stator core oversizing, with a great increase of the track cost. For this reason, we look for that particular value of σ_δ which ensures flux equilibrium.

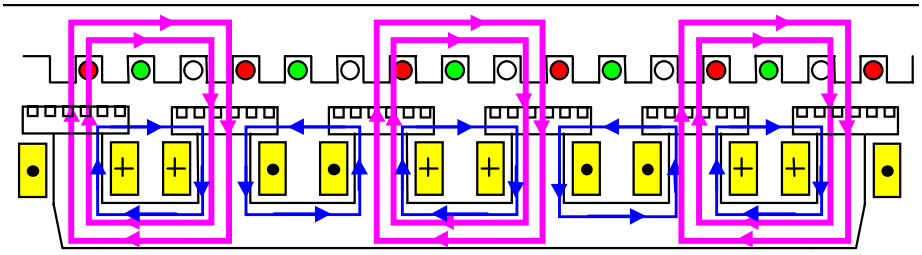

Fig. 2.1.1: fluxes paths in the "independent magnetic loop" operating mode.

On the basis of these aims, we decided that all coils must be equal, and we fixed two conditions: 1) the air-gap flux in the lateral pole shoes is the half that of the central pole shoes; 2) at rated air-gap, levitation force value equals the rated one. These two conditions give two equations in which the only unknown parameters are σ_δ and ℓ: the correction coefficients depend on the dimensions of the air-gap geometry, some of which are known (see tab. 1.1 and 1.2 in Parag.1), and the others are σ_δ and ℓ: thus, the corrective coefficients can be expressed in terms of σ_δ and ℓ; on the other hand, the flux density B_i has to be fixed, and so it is known, too. Finally, we can write a system to obtain the values of σ_δ and ℓ which satisfy the desired conditions.
In the following, we show the used expressions.
For the design stage, only two correction coefficients are considered, one for the lateral poles and the other for the central poles (conversely, for the check analysis stage, each half–polar shoe has an its own correction coefficient). Indicating with the subscripts "*lat*" and "*cent*" the quantities referred to lateral and central pole shoes respectively, the fluxes can be expressed as:

$$\phi_{\delta.lat} = B_i \sigma_\delta A_{geom} k_{\varphi.lat} \qquad \phi_{\delta.cent} = B_i A_{geom} k_{\varphi.cent},$$

therefore, the first condition $\phi_{\delta.lat} = \frac{1}{2}\phi_{\delta.cent}$ is expressed by $\boxed{\sigma_\delta k_{\varphi.lat} = \frac{1}{2} k_{\varphi.cent}}$.

The air-gap levitation force can be expressed as the sum of the forces of each of the 6 levitator poles:

$$F = \sum \frac{1}{2\mu_0} B_i^2 A_{geom} k_F = \frac{1}{2\mu_0} B_i^2 A_{geom} \left(4 k_{F.cent} + 2\sigma_\delta k_{F.lat}\right).$$

As $A_{geom} = b_e \cdot \ell$, and $B_i = B_\delta / k_\varphi$, the force expression becomes

$$F_n = \frac{1}{2\mu_0} \cdot \left(\frac{B_\delta}{k_{\varphi.cent}}\right)^2 \cdot b_e \cdot \ell \cdot \left(4 \cdot k_{F.cent} + 2 \cdot \sigma_\delta \cdot k_{F.lat}\right) \quad \Rightarrow \quad \boxed{F_n = \frac{1}{2\mu_0} \cdot B_\delta^2 \cdot b_e \cdot \ell \cdot \frac{4 \cdot k_{F.cent} + 2 \cdot \sigma_\delta \cdot k_{F.lat}}{k_{\varphi.cent}^2}}.$$

Once chosen B_δ, remembering that the correction coefficients depend on σ_δ and ℓ only, it is possible verify that these are the only unknowns.
With the value $B_\delta = 0.55$ T, from the solution of the two previous equations, it follows: $\sigma_\delta = 0.4$, $\ell = 62$ mm.

2.1.2 Check of the Operated Choices.

The value $\ell = 62$ mm, obtained from (*), is close to $\ell_{sim} = 60$ mm, previously obtained by (**), based on the similitude theory (in which the correction coefficients were neglected):

$$\ell = \frac{F_n}{\left(B_\delta^2 / 2\mu_0\right) \cdot b_e} \cdot \frac{k_{\varphi.cent}^2}{4 \cdot k_{F.cent} + 2 \cdot \sigma_\delta \cdot k_{F.lat}}, \qquad (*) \qquad \ell_{sim} = F \Big/ \frac{1}{2\mu_0} B_\delta{}^2 b. \qquad (**)$$

Also the value $\sigma_\delta = 0.4$ matches the previous analyses [8], which showed that the better flux uniformity was obtained with $\sigma_\delta \approx 0.5$: in these analyses, an ideal circuit without leakage was considered, and the value 0.5 is consistent with this hypothesis. On the contrary, with the present approach, the fringing fluxes are taken into account: this fact increases the equivalent air-gap area, and thus it is reasonable that, with the same air-gap geometry, the same force value is obtained by a lower σ_δ value.
Besides, other literature data ([6, page 314], [7]) show that a value $\sigma_\delta \approx 0.75$ was chosen in the Transrapid project: it is a value significantly greater than 0.5 (theoretical value to obtain stator yoke fluxes equilibrium).
Therefore, we decided to better analyse these three solutions ($\sigma_\delta = 0.4, 0.5, 0.75$): in particular, we considered two levitator positions (position 1: pole axis aligned with stator tooth axis; position 2: pole axis aligned with stator slot axis), and for each of the three solutions we calculated, by FEM analysis, both fluxes distribution in stator yoke (in both positions) and the force variation when passing from one position to the other. The FEM simulation results are shown in Table 2.1.1.
As expected, the choice $\sigma_\delta = 0.4$ leads to a better fluxes equilibrium compared with $\sigma_\delta = 0.5$; nevertheless, we observed that $\sigma_\delta = 0.4$ causes a greater force variation between the two positions; the choice $\sigma_\delta = 0.75$ instead, is unfavourable for both the fluxes imbalance and the force variation.
As a consequence, we decided to adopt $\sigma_\delta = 0.5$, also considering that, even if our platform is static, in a real vehicle a great force fluctuation would represent another difficulty for the levitation control system, as well as an inevitable degradation of the travel comfort.
In these preliminary FEM analysis, the adopted core geometry was characterised by section area of the polar bodies equal to one half of that of the polar shoes, and the stator and levitator yokes section areas were assumed one half of the polar bodies.

Table 2.1.1: FEM simulation results for the considered values of σ_δ; yokes numbering is shown in the figure.

σ_δ	POSIT.	Yoke Fluxes [mWb/m]					Yoke Flux / flux mean value (1)				
		YOKE 1	YOKE 2	YOKE 3	YOKE 4	YOKE 5	YOKE 1	YOKE 2	YOKE 3	YOKE 4	YOKE 5
0.4	1	23.874	19.025	23.313	19.025	23.874	1.094	0.872	1.068	0.872	1.094
	2	22.674	18.947	22.159	18.949	22.673	1.076	0.899	1.051	0.899	1.076
0.5	1	25.819	17.164	25.139	17.165	25.821	1.162	0.772	1.131	0.772	1.162
	2	26.995	14.83	26.2	14.834	26.995	1.229	0.675	1.193	0.675	1.229
0.75	1	32.85	10.42	31.754	10.42	32.852	1.388	0.44	1.342	0.44	1.389
	2	36.693	5.534	35.326	5.535	36.695	1.532	0.231	1.475	0.231	1.532

(1): mean value is the mean of the values in the five yokes.

σ_δ	FORCES [N/m]		(f1-f2) / f1
	f1	f2	
0.4	39890	36940	0.074
0.5	40110	39240	0.022
0.75	42110	44050	-0.046

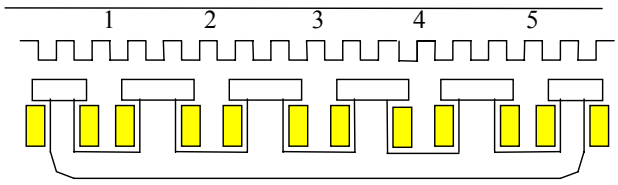

f1 = force in position 1 (pole axis – tooth axis); f2 = force in position 2 (pole axis – slot axis)

Table 2.1.1 is interesting also because it shows the size of flux and force variations between the two extreme positions (1 and 2): considering the flux, the variation increases with the increase of σ_δ, while as regards the force, the variation has a minimum for $\sigma_\delta = 0.5$, then it increases both if σ_δ increases and lowers.
Finally, we notice that, with the choice $\sigma_\delta = 0.5$, the air-gap geometry is completely defined: this allows to calculate the value of all the correction coefficients, for any air-gap value (in particular, for rated air-gap).

2.1.3 Estimation of the Other Magnetic Circuit Dimensions.

Once defined the air-gap geometry, we have to calculate all the other magnetic structure dimensions.
First of all, known the exact expressions of the correction coefficients, we can calculate the value of B_i effectively needed to produce the desired force, by the following expression:

$$F = \left(4 \cdot k_{F.cent} + 2 \cdot \sigma_\delta \cdot k_{F.lat}\right) \cdot A_{ge\,om} \cdot B_i^2 \,/ 2\mu_0 \;;$$

once known B_i, the air-gap flux $\varphi_\delta = B_i A_{ge\,om} k_\varphi$ and the magnetic voltage $U_\delta = \left(B_i / \mu_0\right) \cdot \delta$ are evaluated.
Once calculated the air-gap fluxes, we can obtain an estimate of the polar bodies section area, useful to evaluate the size of the coil width; this quantity, together with the rated air-gap magnetic voltage $U_{\delta n}$, allows

to calculate the size of the coil height, and so the polar bodies height.
At this time, geometrical leakage reluctances can be calculated.

Then, the air-gap reluctances are evaluated, by using this kind of expressions: $\theta_\delta = \dfrac{\delta}{\mu_0 \cdot A_{geom} \cdot k_\varphi}$.

Once known all the "in air"-reluctances (air-gap and leakage), and neglecting for now the core reluctances, the magnetic network is solved (fig. 2.1.2), and the flux in each branch is calculated; chosen in advance the value of the rated core flux density (B_{fe} = 1.4 T), the design can be completed, calculating the section area of every branch. The obtained values are as follows: central polar bodies width = 42 mm; lateral polar bodies width = levitator yoke height = 21 mm; stator yoke height = 18 mm.

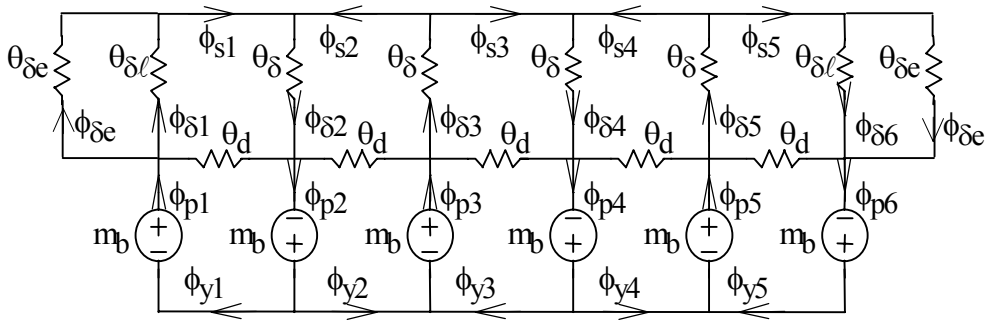

Fig. 2.1.2: magnetic equivalent network of the levitator with coils only.

- ϕ_s , ϕ_y , ϕ_δ , ϕ_p *indicate respectively fluxes in stator yokes, levitator yokes, air-gaps, poles;*
- θ_δ , $\theta_{\delta\ell}$, $\theta_{\delta e}$, θ_d *indicate central, lateral, external air-gap reluctances, and leakage reluctances.*

2.1.4 Check of the Flux Density Levels During the Lifting Process, through FEM Analysis.

The last step of the design is the flux density evaluation in each section, during lifting process, carried out by FEM analysis, to verify that the core is not saturated (or the saturation level is low); in fact, lifting is the worst condition because, maintaining the same air-gap flux (and thus, roughly the same levitation force), if the air-gap increases, leakage increases too, and thus also the flux in the levitator yokes rises. In this analysis, we considered the actual lamination B(H) curve (removing the previously adopted hypothesis $\mu_{fe} = \infty$).
The result of this test was positive, therefore the dimensions considered so far are assumed as ultimate ones.
Fig. 2.1.3 shows the main dimensions, while fig. 2.1.4 shows a photo of the constructed levitator prototype.

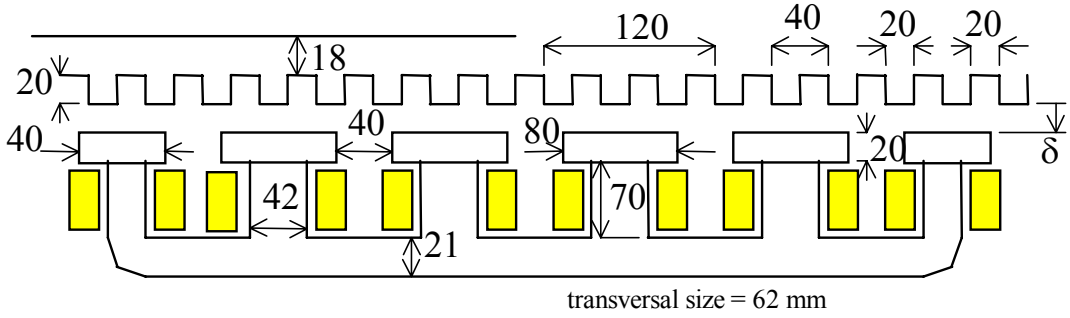

Fig. 2.1.3: main dimensions (in mm) of the constructed prototype of the levitator with coils only.

Fig. 2.1.4: photograph of the constructed prototype of the levitator with coils only.

2.2 Design Procedure of the Permanent Magnet of the Hybrid Levitator.

The material chosen for the permanent magnet (PM) is NdFeB, with remanence equal to B_r = 1.18 T and coercive force H_0 = – 800 kA/m; the recoil characteristic is very linear, hence we assumed it is a straight line with slope equal to the recoil permeability $\mu_{rev} = \mu_r \mu_0 = B_r / H_0$ (with μ_r = relative recoil permeability).
The design aim is to find the PM area A_m and height h_m; as we assume that the PM transversal size equals the levitator transversal dimension ℓ, the definition of the PM area means choosing its longitudinal width b_m.
In the design stage, we assume that the six levitator branches operate in the same manner: thus, a circuit with only one of these branches will be considered; the corresponding equivalent circuit is shown in fig. 2.2.1.

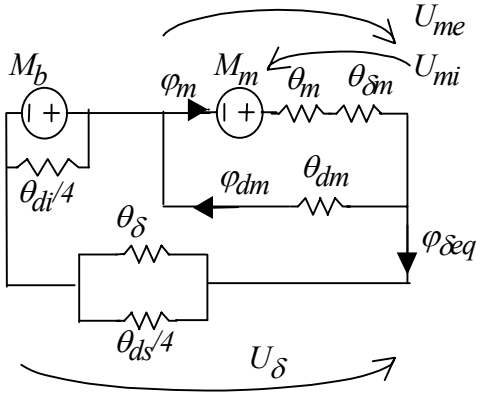

M_m, M_b = PM and coil m.m.f.;
θ_m, $\theta_{\delta m}$, θ_{dm} = internal, air-gap(♣), and leakage reluctances of PM;
θ_δ = air-gap reluctance;
θ_{di}, θ_{ds} = lower (i) and upper (s) leakage reluctances;
φ_m, φ_{dm} = PM total and leakage fluxes;
H_o, B_r = PM coercive force and remanence;
μ_r = PM relative recoil permeability;
h_m, b_m, ℓ = PM height, width and transversal size;
B_m = PM working flux density.

(♣): we call "PM air-gap reluctances" the reluctance of the clearance between the magnet and the plates among which it is inserted.

Fig. 2.2.1: equivalent circuit for the PM design.

The PM characteristics are related to the circuit parameters as follows (B_m = working PM flux density):

$$M_m = H_0 h_m \qquad \varphi_m = B_m A_m = B_m \ell b_m \qquad \theta_m = \frac{h_m}{\mu_r \mu_0 \ell b_m} \qquad \theta_{\delta m} = \frac{\delta_m}{\mu_0 \ell b_m} \quad ; \tag{1}$$

the expressions of θ_{dm} and θ_{di} are reported in [5].

The unknown dimensions b_m and h_m only derive from coil and PM working conditions, that is from coil m.m.f. M_b and PM flux density B_m, because, once fixed these quantities, the height h_m follows from the PM magnetic voltage law (UL): $M_m = U_{mi} + U_{me}$, while the width b_m comes out from the PM fluxes law at the knot (ΦL): $\varphi_m = \varphi_{dm} + \varphi_{\delta eq}$. In fact:

$$U_{mi} = (\theta_m + \theta_{\delta m})\varphi_m = \left(\frac{h_m}{\mu_r \mu_0 \ell \cdot b_m} + \frac{\delta_m}{\mu_0 \ell \cdot b_m} \right) B_m \ell \cdot b_m = \left(\frac{h_m}{\mu_r \mu_0} + \frac{\delta_m}{\mu_0} \right) B_m ,$$

$$U_{me} = U_\delta - M_b , \qquad \varphi_{dm} = \frac{U_{me}}{\theta_{dm}} , \qquad \varphi_{\delta eq} = U_\delta \left(\frac{1}{\theta_\delta} + \frac{4}{\theta_{ds}} \right) , \qquad M_m = H_0 h_m , \quad \varphi_m = B_m \ell \cdot b_m ,$$

and therefore UL and ΦL yield respectively to:

$$H_0 h_m = \left(\frac{h_m}{\mu_r \mu_0} + \frac{\delta_m}{\mu_0} \right) B_m + U_\delta - M_b , \qquad B_m \ell_e b_m = \frac{U_{me}}{\theta_{dm}} + U_\delta \left(\frac{1}{\theta_\delta} + \frac{4}{\theta_{ds}} \right) ; \tag{2}$$

we see that, once fixed M_b and B_m, the only unknown are h_m and b_m.

Working conditions could be chosen arbitrarily; we decided to do as follows:

- we defined the two ratios, with tight reference to the rated operating conditions (rated air-gap and load):
  - ρ = ratio between rated values of coil m.m.f. M_{bn} and total air-gap magnetic voltage $U_{\delta n}$: $\rho = M_{bn} / U_{\delta n}$;
  - χ = ratio between rated values of PM working flux density B_{mn} and remanence B_r: $\chi = B_{mn} / B_r$;
  these parameters can be regarded as working coefficients of coil and PM respectively; subscript "n" indicates that both are referred to rated conditions;
- we fixed three minimisation goals, and wrote objective functions to express these goals; in particular:
  1. Joule losses in the windings, and therefore RMS value of coil m.m.f.;
  2. PM volume;
  3. "gluing" force, that is attractive force when air-gap is 1/10 of rated value and coil current is absent;

- we looked for parameters values $\bar{\rho}$, $\bar{\chi}$ which meet the previously defined goals;
- finally, by (2), PM dimensions b_m, h_m were expressed as a function of the parameters ρ, χ, yielding to

$$h_m = \delta_m \frac{\mu_r \chi}{1-\chi} + \frac{1-\rho}{1-\chi}\frac{U_{\delta n}}{H_0}, \qquad b_m = \frac{U_{\delta n}}{\chi H_0 \mu_r \mu_0 \ell}\left(\frac{1}{\theta_{\delta n}} + \frac{4}{\theta_{ds}} + \frac{1-\rho}{\theta_{dm}}\right) \tag{3}$$

  and the dimensions related to $\bar{\rho}$, $\bar{\chi}$ values were calculated.

These chosen goals need some explanations.
In a hybrid PM levitator, the main problem is that, due to PM presence, a failure in the coil feeding system does not lead to the levitation force zeroing (as happens in a levitator with coils only): so, if the failure happens in an instant when the air-gap is lower than its rated value, the vehicle does not tend to lean down on the track, but to glue up to it, with a consequent irreversible damage of the whole system (the landing on the track is less harmful, thanks to the usual presence of special sliding blocks): this is the reason why it was decided to minimise the "gluing" force, and why we analysed the condition of reduced air-gap and zero current. Of course, the heaviness of the "gluing" effect is related not only to the air-gap value, but also to the levitator vertical speed while approaching that value; however, we only analysed static conditions, considered as an index of the gluing risk.

Remembering that the coil m.m.f. equals the product of current density times the net copper area, the Joule losses can be expressed as a product of resistivity, current density, turn average length and m.m.f.:

$$P = \rho_{Cu} \cdot J^2 \cdot Vol = \rho_{Cu} \cdot J^2 \cdot \ell \cdot A_{Cu} = \rho_{Cu} \cdot J \cdot \ell \cdot J \cdot A_{Cu} = \rho_{Cu} \cdot J \cdot \ell \cdot fmm\,.$$

Considering that the polar bodies section area will be only slightly different from that of the levitator with coils only, the turn average length can be considered known and constant; current density and resistivity are known, too: thus, the losses are directly proportional to the coil m.m.f..
In the following, we show how we expressed the objective functions.

Magnet volume.
This is the easiest function to formulate, because the volume is simply the product of the PM dimensions:

$$V_m = h_m b_m \ell = \left(\delta_m \frac{\mu_r \chi}{1-\chi} + \frac{1-\rho}{1-\chi}\frac{U_{\delta n}}{H_0}\right)\frac{U_{\delta n}}{\chi H_0 \mu_r \mu_0 \ell}\left(\frac{1}{\theta_{\delta n}} + \frac{4}{\theta_{ds}} + \frac{1-\rho}{\theta_{dm}}\right)\cdot \ell = V_m(\rho,\chi)\quad .$$

If we fix some values of ρ as a parameter and we let χ change, we can analyse the PM volume as a function of χ, as shown in fig. 2.2.2; concerning this diagram, we note that:
- to consider a dimensionless quantity, we plotted the ratio $vol_m(\rho, \chi) = V_m(\rho, \chi) / V_m(0{,}0.5)$;
- the range is limited to $\chi > 0.5$, because adopting $\chi < 0.5$, where the function has a symmetrical shape, leads to work in the lower zone of PM characteristic, where irreversible demagnetization risks increase;
- the plot ends in $\chi = 0.9$, as $\chi = 1$ is an asymptotic limit (if $\chi \to 1$, PM height tends to infinite, while the section area assumes a finite value, hence volume rises to infinite; the asymptotic trend occurs even if $\chi \to 0$: in this case, the opposite happens: PM height assumes a finite value and section area tends to infinite);
- we notice that nearby the value $\chi = 0.5$, which minimises the PM volume, the function is rather flat: this means that even if we move from this value, in the proximity we do not have a great volume rise;
- we also notice that, with the same value of χ, the volume diminishes at the rise of ρ: this can be explained considering that if the coil m.m.f. portion increases, the m.m.f. portion given by the PM decreases.

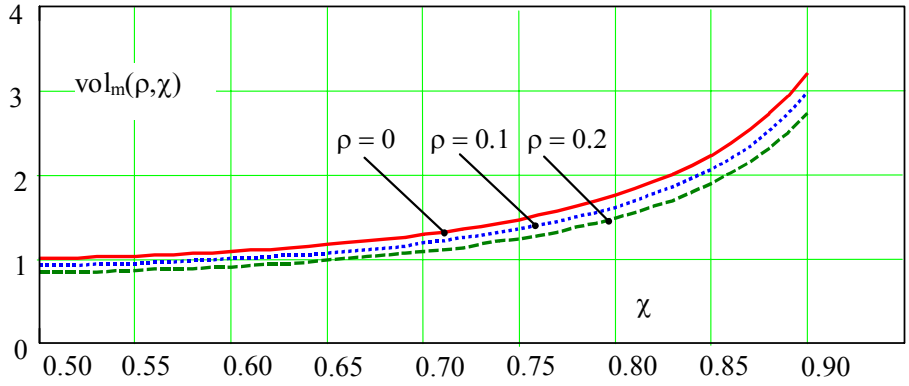

Fig. 2.2.2: diagram of the p.u. PM volume, as a function of χ, for different values of the parameter ρ .

Gluing force.
It can be calculated by means of the following expression:

$$F = \sum \frac{\mu_0}{2} \cdot \left(\frac{U_\delta}{2} \right)^2 \cdot b_e \cdot \ell \cdot k_F = \sum \frac{\mu_0}{2} \cdot \left(\frac{U_\delta}{2} \right)^2 \cdot b_e \cdot \ell \cdot \left(4 \cdot k_{F.cent} + 2 \cdot \sigma_\delta \cdot k_{F.lat} \right) \quad , \tag{4}$$

in which the air-gap magnetic voltage U_δ must be expressed as a function of the parameters ρ, χ . To do so, the circuit shown in fig. 2.2.1 is solved, yielding:

$$U_\delta = \frac{M_m + M_b \left(1 + \frac{\theta_m + \theta_{\delta m}}{\theta_{dm}} \right)}{1 + (\theta_m + \theta_{\delta m}) \left(\frac{1}{\theta_\delta} + \frac{4}{\theta_{ds}} + \frac{1}{\theta_{dm}} \right)} = \frac{H_0 h_m + \rho U_{\delta n} \left(1 + \frac{\theta_m + \theta_{\delta m}}{\theta_{dm}} \right)}{1 + (\theta_m + \theta_{\delta m}) \left(\frac{1}{\theta_\delta} + \frac{4}{\theta_{ds}} + \frac{1}{\theta_{dm}} \right)} \quad ; \tag{5}$$

we note that θ_m and $\theta_{\delta m}$ depend on b_m and h_m, and so they depend on ρ, χ.
In the "gluing" condition, the coil m.m.f. is zero ($M_b = 0$), the air-gap assumes the gluing value ($\delta = \delta_{glue} = 0.1 \cdot \delta_n$, due to the contact mechanical clearance) and PM leakage is nearly absent ($\theta_{dm} \to \infty$), thus we have:

$$U_{\delta.inc} = \frac{H_0 h_m}{1 + (\theta_m + \theta_{\delta m}) \left(\frac{1}{\theta_{\delta.inc}} + \frac{4}{\theta_{ds}} \right)} \quad .$$

We adopt the approximation $k_{F.lat} = k_{F.cent}$, in such a way that the expression $4 \cdot k_{F.cent} + 2 \cdot \sigma_\delta \cdot k_{F.lat}$ can be simplified to $5 \cdot k_{F.cent}$. In conclusion, the gluing force expression becomes:

$$F_{inc} = \frac{\mu_0}{2} \cdot \left(\frac{U_{\delta.inc}}{\delta_{inc}} \right)^2 \cdot b_e \cdot \ell \cdot 5 \cdot k_{F.cent} \qquad \text{with} \quad U_{\delta.inc} = \frac{H_0 h_m}{1 + (\theta_m + \theta_{\delta m}) \left(\frac{1}{\theta_{\delta.inc}} + \frac{4}{\theta_{ds}} \right)} \quad ,$$

where θ_m and $\theta_{\delta m}$ depend on b_m and h_m through (1), b_m and h_m are expressed as functions of ρ, χ through (3). If we fix some values of ρ as a parameter and we let χ change, we obtain the gluing force as a function of χ, as shown in fig. 2.2.3; concerning this diagram, we note that:
- to consider a dimensionless quantity, we plotted the ratio $\gamma(\rho, \chi) = F_{inc}(\rho, \chi) / F_{nom}$;
- the highest force values are not realistic, as force is limited by core saturation;
- the plot has been truncated in $\chi = 0.1$, as the value $\chi = 0$ is an asymptotic limit (ideally, if $\chi \to 0$, PM section area tends to infinite, and so the force does the same; if $\chi \to 1$ instead, there is a finite force value, because, as PM height rises to infinite, both PM m.m.f. and its internal reluctance increase).

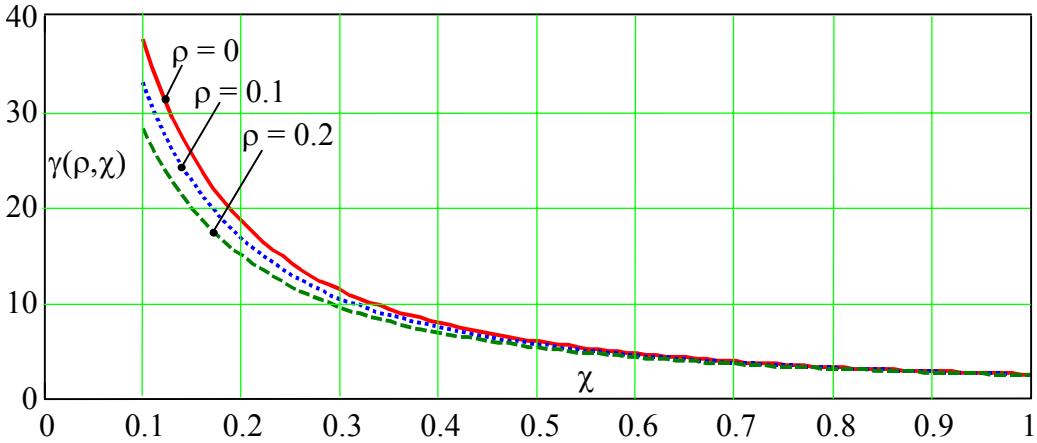

Fig. 2.2.3: diagram of p.u. gluing force as a function of χ, for different values of the parameter ρ.

For low χ values, the force diminishes when ρ increases: this can be explained by observing that, as ρ increases, the PM mass decreases and (within the range $\chi < 0.5$) the PM section area diminishes too (attraction force is directly proportional to the PM section area, therefore the former decreases together with the latter). For high χ values, the PM height is so high that the contribution of the coil m.m.f. cannot affect the force value anyway: due to this fact, as χ approaches 1, the force becomes independent on the ρ value.

RMS Value of the Coil m.m.f.

To estimate this value, we need to know the time waveform of the m.m.f.; about this, we note that, as the air-gap changes, the control system regulates the m.m.f. in such a way to maintain the levitation force constant: thus, the m.m.f. $m_b(t)$ can be regarded as the sum of a constant value $\rho \cdot U_{\delta n}$ and of an alternative term, changing in frequency and amplitude as a consequence of the instantaneous air-gap fluctuations; the constant value is called "biasing m.m.f." M_p, while the alternative term can be defined the "regulation m.m.f." $m_r(t)$: $m_b(t) = M_p + m_r(t) = \rho \cdot U_{\delta n} + m_r(t)$. On the basis of this decomposition it follows that the global RMS value squared of the total m.m.f. equals the sum of the RMS values squared of the two components of $m_b(t)$.

Now we have to suppose the time waveform of the regulation m.m.f.. For a rough estimate, we can assume that it consists of sinusoidal half-waves, defined as follows: we can suppose that the positive peak amplitude equals the m.m.f. required for an air-gap equal to the highest one allowed by the control system (1.5 times the rated air-gap δ_n), while the negative peak amplitude equals the m.m.f. needed for an air-gap equal to the lowest allowed (one half of δ_n); as the m.m.f. – air-gap characteristic is not linear, the two amplitudes are different each other, and so positive and negative half-waves are different: in conclusion, the supposed waveform of the regulation m.m.f. versus time is depicted in fig. 2.2.4.

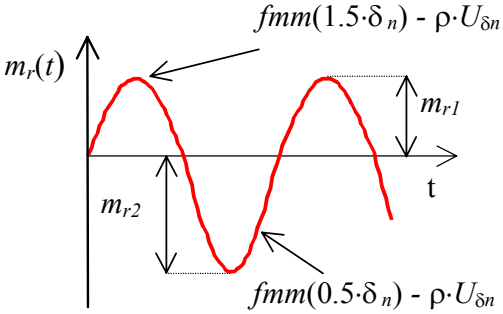

Fig. 2.2.4: diagram of the supposed time waveform of the regulation m.m.f..

If the analytical expression of this function is

$$m_r(t) = \begin{cases} m_{r1}\,\mathrm{sen}(\omega t) & 2k\pi < \omega t < (2k+1)\pi \\ m_{r2}\,\mathrm{sen}(\omega t) & (2k+1)\pi < \omega t < 2(k+1)\pi \end{cases},$$

the RMS value M_b of the whole m.m.f. $m_b(t)$ equals:

$$M_b = \sqrt{{M_p}^2 + \frac{{m_{r1}}^2 + {m_{r2}}^2}{4} + \frac{2}{\pi} M_p (m_{r1} - m_{r2})}\,.$$

Now, we need to express the instantaneous value of the regulation m.m.f. as a function of the parameters ρ, χ. In order to operate this transformation, we proceed as follows:

- from equation (5) (air-gap magnetic voltage U_δ as a function of ρ, χ) we get the expression of the coil total m.m.f. M_b as a function of ρ, χ, U_δ, obtaining:

$$M_b = U_\delta \left(1 + \frac{\frac{1}{\theta_\delta} + \frac{4}{\theta_{ds}}}{\frac{1}{\theta_m + \theta_{\delta m}} + \frac{1}{\theta_{dm}}} \right) - H_0 h_m \frac{1}{1 + \frac{\theta_m + \theta_{\delta m}}{\theta_{dm}}} \quad ; \qquad (6)$$

- equating the force expression (4) to the rated force value F_n, we get the expression of the magnetic voltage required to produce the rated force value (with any air-gap)

$$U_\delta = \delta \cdot \sqrt{\frac{2F_n}{\mu_0 b_e \cdot \ell \cdot (4 \cdot k_{F.cent} + 2 \cdot \sigma_\delta \cdot k_{F.lat})}} \quad ; \qquad (7)$$

- putting (7) in (6) we obtain the expression of the m.m.f. value that the coil has to produce in such a way to obtain the desired force value;
- subtracting the biasing m.m.f. $M_p = \rho \cdot U_{\delta n}$ from the total m.m.f. M_b (both depending on ρ, χ, δ), we obtain also the regulation m.m.f. as a function of ρ, χ, δ:

$$m_r(\delta, \rho, \chi) = \delta \cdot \sqrt{\frac{2F_n}{\mu_0 b_e \ell \cdot (4 \cdot k_{F.cent} + 2 \cdot \sigma_\delta \cdot k_{F.lat})}} \cdot \left(1 + \frac{\frac{1}{\theta_\delta} + \frac{4}{\theta_{ds}}}{\frac{1}{\theta_m + \theta_{\delta m}} + \frac{1}{\theta_{dm}}} \right) - H_0 h_m \frac{1}{1 + \frac{\theta_m + \theta_{\delta m}}{\theta_{dm}}} - \rho U_{\delta n}\,;$$

- finally, evaluating $m_r(\delta, \rho, \chi)$ for $\delta = 0.5 \cdot \delta_n$ and $\delta = 1.5 \cdot \delta_n$, we have the two expressions of m_{r1} and m_{r2} (as a function of ρ, χ), needed to calculate the RMS value of total m.m.f..

If we fix some values of ρ as a parameter, and we let χ change, we obtain the RMS value of total m.m.f. as a function of χ, as shown in fig. 2.2.5; in order to consider a dimensionless quantity, we plotted the function $(M_b(\rho, \chi) / U_{\delta n})^2$, defined $m_{t.q}(\rho, \chi)$, which is the squared value of the ratio among the total m.m.f. (biasing + regulation) and the rated air-gap magnetic voltage.

We note that as χ increases, the m.m.f. increases too: this happens because as the PM height rises, its reluctance increases, and hence the equivalent reluctance seen by coil rises too; we also notice that the m.m.f. value is almost independent from the ρ value.

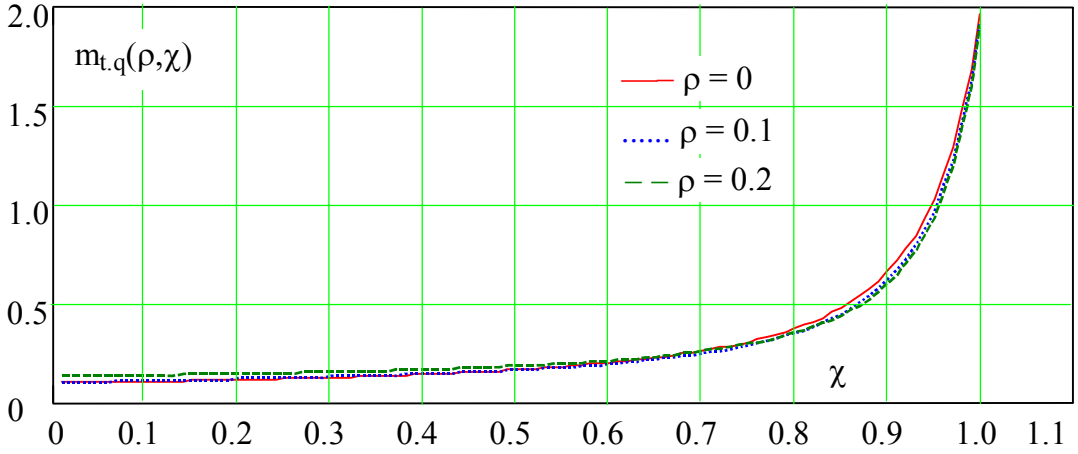

Fig. 2.2.5: diagram of the RMS value of the total m.m.f. as a function of χ , for different ρ values.

As could be predictable, the three aims are gained by range of values different from each other: each function is minimized by a range of values which does not minimise the two others; in fact, it was possible to predict that these aims are conflicting: a reduction of gluing force is only gained by using a high value of ρ, in such a way to reduce the PM m.m.f., but this leads to an increase of coil losses; the PM volume reduction needs a rise of ρ, too. Therefore, we decided to assume as basic criteria 1) losses minimisation, which leads to assume $\rho = 0$, and 2) optimized PM sizing, which leads to $\chi = 0.55$, even if these choices result in a quite high value of the static gluing force (ideally about 5 times the rated force value). This is a hard condition for the control system, because the higher is the gluing force, the faster must be the system response; nevertheless, as this is a prototype, we think worthwhile to test the worst condition: if we gain a stable system in this case, it is likely to obtain a correct operation even with more favourable conditions, that is with higher values of ρ and χ (putting $\rho \neq 0$, that is introducing a biasing m.m.f., on the one hand reduces the gluing risk, because it increases the probability that, in case of failure, the vehicle lies down on the track; on the other hand, it reduces the amount of levitation force given by the PM, and so it reduces also the energy involved in the collision in case of gluing). We add that the p.u. gluing force equals 5 only in the ideal case of infinite core permeability: in the actual case, the core saturation surely limits the gluing flux density and thus the force.
We therefore assume $\rho = 0$ and $\chi = 0.55$.

2.3 Hybrid Levitator Design.

2.3.1 Definition of the Structure Geometry at the Air-gap.

As previously said, for the hybrid levitator we assume the same air-gap geometry of the levitator with coils only: this choice leads to the same values of the parameters σ_δ and ℓ, of the correction coefficients, of the air-gap reluctances, of the quantities B_i and $U_{\delta n}$, and therefore of the air-gap fluxes.

2.3.2 Calculation of the Geometrical Leakage Reluctances.

We proceed in the same way as for the levitator with coils only: once known the air-gap flux, we can give an estimate of the polar bodies sections, from which the coil width can be evaluated; this value, together with the required coil m.m.f. value, allows to calculate the coil height, from which the polar bodies height is obtained; in this way, the geometrical leakage reluctances can be evaluated. Differently from the case with coils only, where the m.m.f. was equal to $U_{\delta n}$, here the m.m.f. is not known yet, as it depends on the PM dimensions, not chosen yet: as a first choice, we suppose that the m.m.f. is about half the $U_{\delta n}$ value.

2.3.3 Definition of the PM Dimensions.

Once the air-gap geometry is known and the leakage reluctances are estimated, we apply the previously described method to size the PM; with the adopted choice ($\rho = 0$, $\chi = 0.55$) we obtain: $b_m = 76$ mm; $h_m = 6$ mm.

2.3.4 Evaluation of the Section Areas.

We proceed in the same manner adopted for the levitator with coils only: we solve the simplified circuit (fig. 2.3.1), calculating the fluxes in all the branches and, once fixed the working core flux density (again B_{fe} = 1.4 T), we evaluate the section area needed to carry these fluxes. The obtained values are: central polar bodies width = 38 mm; lateral polar bodies width = levitator yoke height = 19 mm; stator yoke height = 18 mm.

As regards the check of the flux density levels by FEM analysis, we proceed as done for the levitator with coils only. Also in this case, FEM check of flux densities during the lifting process showed that the core saturation is very limited, thus the previous sizes are assumed as the ultimate ones. Fig. 2.3.2 shows the main dimensions, while fig. 2.3.3 shows a photograph of the constructed prototype of the hybrid levitator.

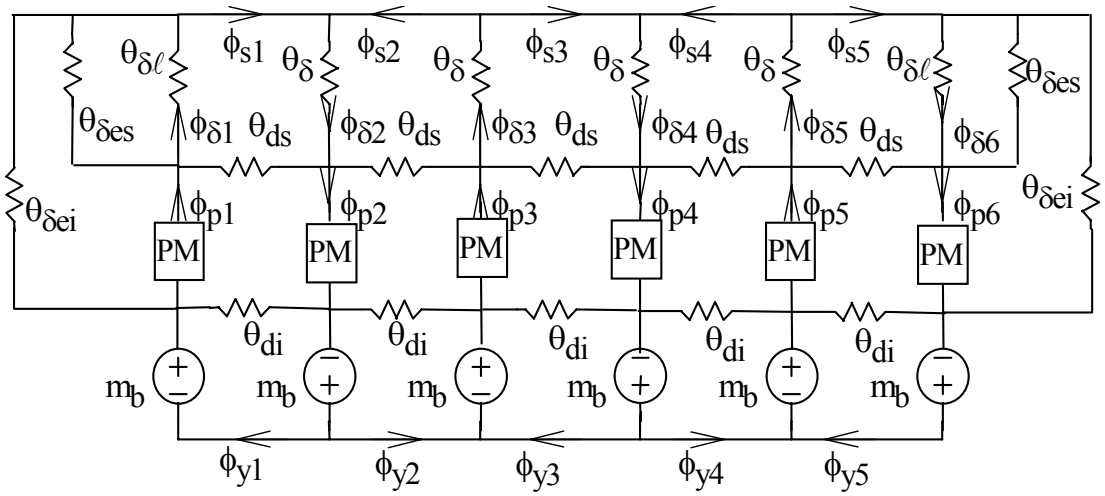

Fig. 2.3.1: magnetic equivalent network of the hybrid PM levitator.

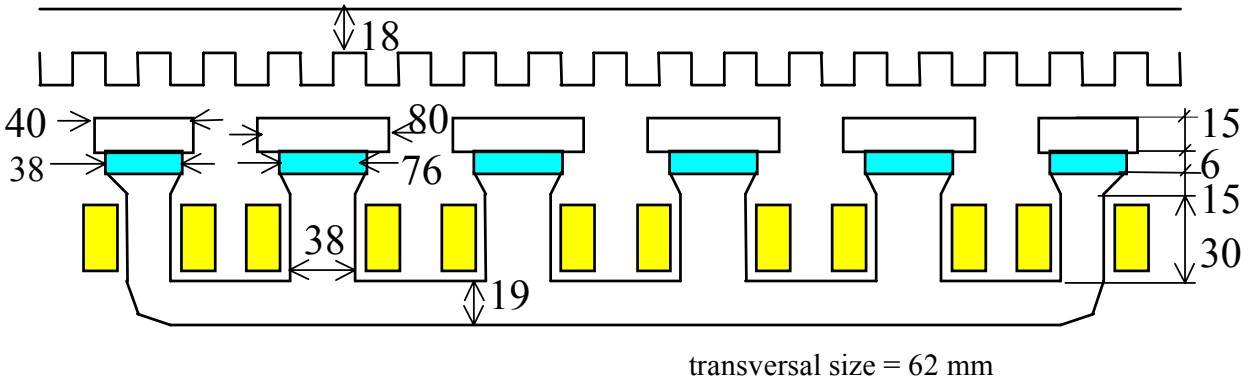

Fig. 2.3.2: main dimensions (in mm) of the designed hybrid PM levitator.

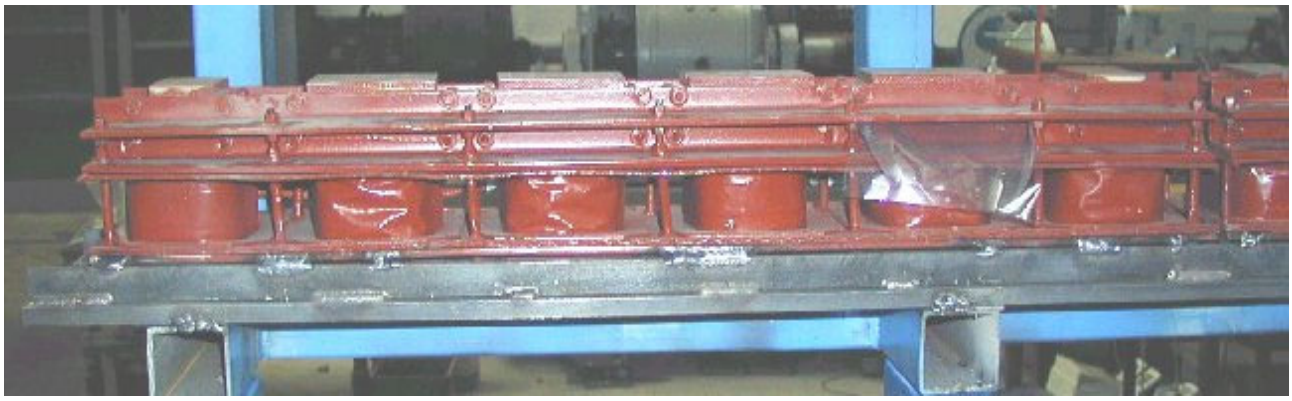

Fig. 2.3.3: photograph of the constructed prototype of the hybrid PM levitator.

3. Conclusions

In the present paper, a method was presented for the design of EMS Maglev vehicle levitators, both that with coils only and hybrid one (with coils and permanent magnets).
The definition of a similitude theory led to define suited criteria for a scaled reduction of force, longitudinal and transversal dimensions and air-gap width, in such a way to make prototypes of reduced sizes, but maintaining the same main physical quantities (air-gap flux density and winding current density) and the same mechanical dynamic of the real systems.
The design procedure is based on a magnetic circuit modelling of the levitation system, in which fluxes and levitation force calculations has been improved by use of correction coefficients, obtained by the analytical solution of the air-gap field.
Referring to the levitator with coils only, the choice was discussed of the esapolar levitator transversal dimension and lateral pole shoe extension, and these choice were checked by circuit and FEM analysis.
About the PM sizing in the hybrid levitator, we analysed how different values of biasing m.m.f. in the coils and different working conditions of the PMs affect three objective functions: coil losses, PM mass and "gluing" force (attractive force for zero current and nearly zero air-gap).
The employment of this design procedure led to the definition of all the levitator dimensions, both in case of a levitator with coils only and in case of a hybrid one; subsequently, the construction of the prototypes has followed.
The activity will proceed, with the levitation platforms testing, in different operating and control conditions.

References

1. A. Di Gerlando, G. Foglia, "Improved analytical evaluation of air-gap fluxes and forces of ferromagnetic smoothed and toothed structures and pole shoes", in International Journal COMPEL, n° 19, 2000.
2. F. Castelli Dezza, A. Di Gerlando, G. Foglia, "Field-circuit integrated methodologies for design and modelling of PM levitation devices for Maglev transportation systems", in International Journal COMPEL, n° 19, 2000.
3. F. Castelli Dezza, A. Di Gerlando, G. Foglia, "Theoretical Studies and Experimental Activities on EMS Levitation Devices for Maglev Levitation Systems", in MAGLEV 2000, Proceedings of the 16th International Conference on magnetically levitated systems and linear drives, June 7-10 2000, Rio De Janeiro, Brazil, pag. 213-218.
4. G. Foglia, "Theoretical and Experimental Analysis of Excitation and Levitation Devices in EMS Maglev Systems ", Ph. D. Thesis c/o Politecnico di Milano, XIII Doctorate Cycle, February 2001.
5. F. Castelli Dezza, A. Di Gerlando, G. Foglia, "Improved Magnetic Modelling of EMS Maglev Levitators", accepted for publication in MAGLEV 2002 Proceedings.
6. I. Boldea, S. A. Nasar, Linear motion electromagnetic system, John Wiley & Sons, 1985.
7. G. W. McLean, "Review of recent progress in linear motors", IEE Proc.-B, vol.135, n.6, November 1988.
8. Piccagli E., Tecchio M., "Design Analysis of Inductors in EMS Maglev Transportation Systems", Laurea Thesis, Politecnico di Milano, A.A. 1995-96.